Electronic Supplementary Material (ESI) for Journal of Materials Chemistry C.

Supporting Information

Improved anisotropy and piezoelectricity by applying in-plane deformation in monolayer WS_2

Ling Li[1], Peiting Wen[2], Yujue Yang[1]*, Nengjie Huo[2]*, and Jingbo Li[2]*

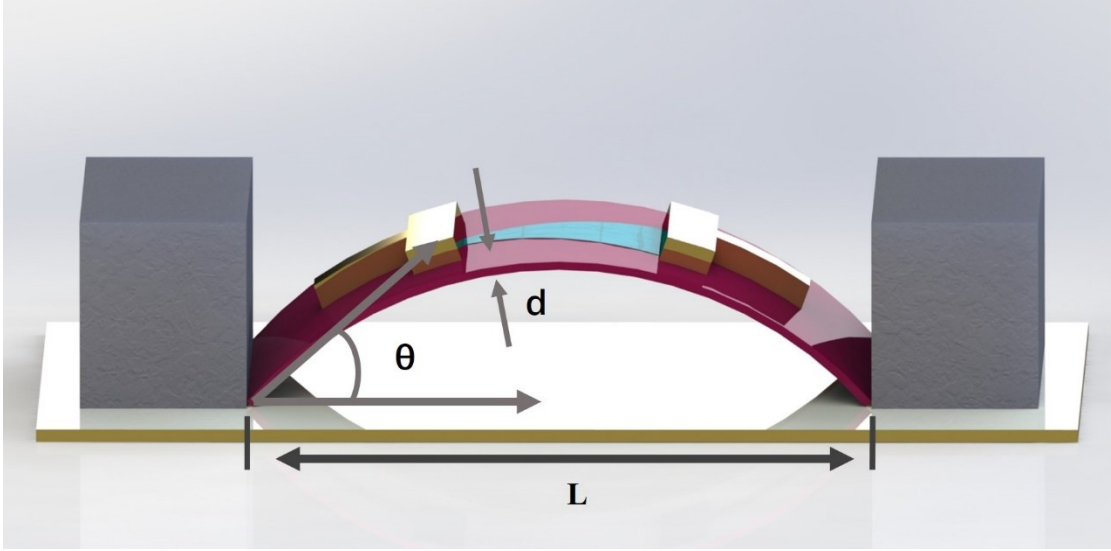

Fig. S1 Schematic diagram of estimating strain in WS_2 device. The applied strain on the substrate deformation can be figured out using the formula $\varepsilon = \frac{d\sin\theta}{L}$, where, ε is the strain, d is The thickness of the substrate, ɵ is the angle between the tangent line at the end of substrate and the horizontal line, L is the length of horizontal line form the one end of substrate to the another end of substrate.[7]

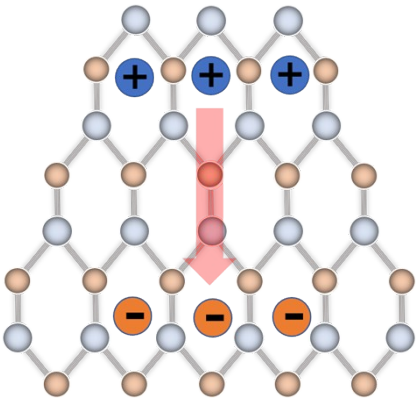

Fig. S2 Schematics of polarization charges and piezoelectric field for the WS_2 with strain along the armchair directions. The piezoelectric charges are distributed at the zigzag end edges.

When the strain is applied on WS_2 along the armchair direction, the W and S atoms will shift from the initial position. The increased length of W-W and W-S bond in that direction can form the electric dipoles which will cause a piezoelectric field along the Armchair direction. Figure S2 shows the distribution of polarization charges in the deformed WS_2, which can cause the piezoelectric effect.

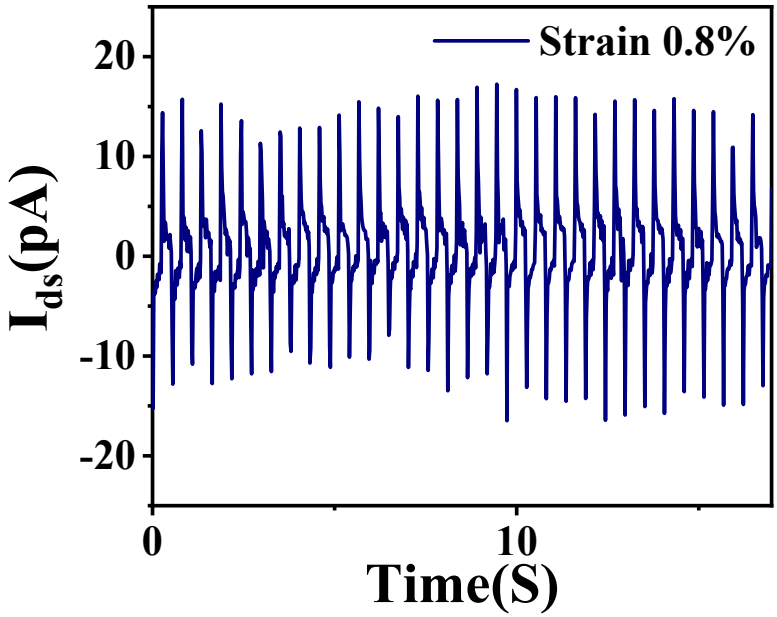

Fig. S3 Dynamic piezoelectric output signal was produced repeatedly after hundreds of cycles under 0.8% strain.

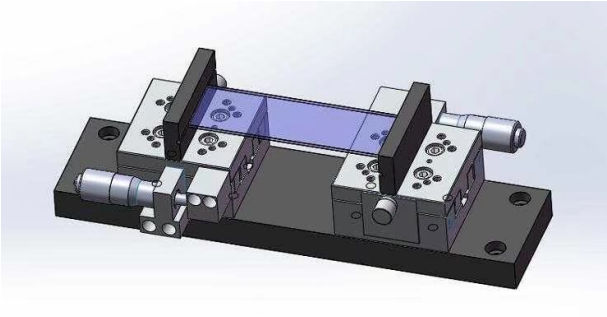

Fig. S4 Schematic diagram of the linear stage used to apply the in-plane uniaxial strain.

For the process of applying uniaxial strain. First, the monolayer WS_2 is transferred to the PDMS substrate, then we in-plane stretch PDMS to introduce the uniaxial strain on WS_2. The linear stage as shown in Fig. S4 is used to stretch PDMS film. The edge sides are fixed on both sides of the linear stage, then move the stage to increase the distance and thus realize the deformation of WS_2. The in-plane strain can vary by changing the distance, Raman and PL spectra are subsequently performed under the different strain conditions.

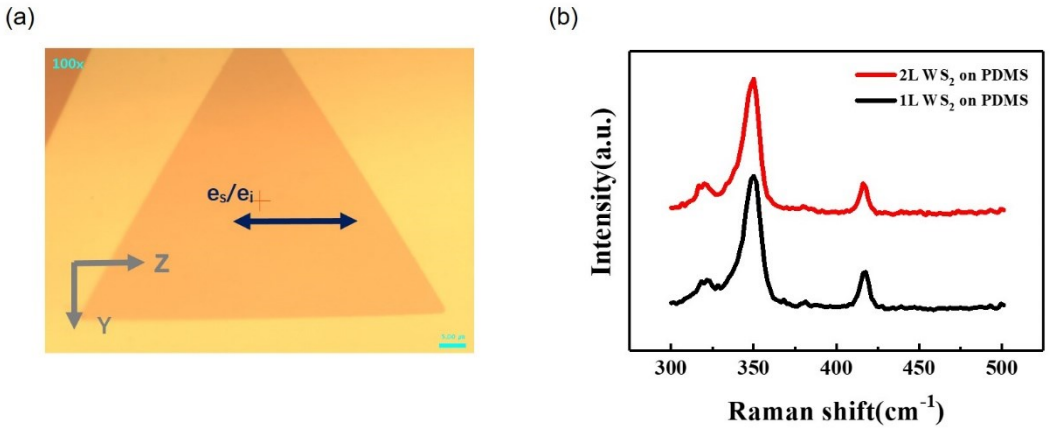

Fig. S5 (a) Optical image of WS_2 device labels the direction of the incident laser and scattered light. (b) The normalized Raman spectrum of 1L/2L WS_2 on PDMS.

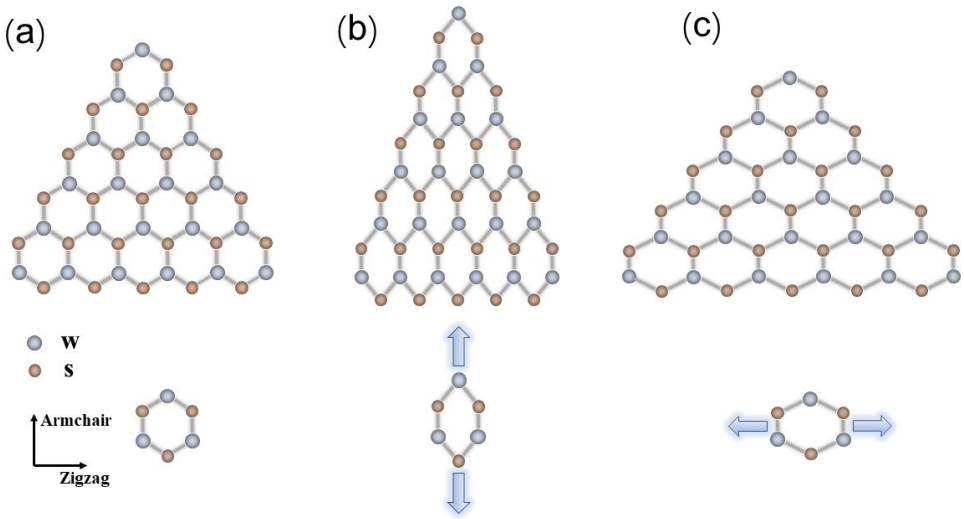

Fig. S6 Atomic structure of monolayer WS_2 for its initial state without strain (a), deformed state with strain along armchair direction (b) and zigzag direction (c).

We have plotted the atomic structures for the pristine WS_2 without strain (Fig. S6a), in-plane deformed WS_2 along the armchair direction (Fig. S6b) and zigzag direction (Fig. S6c). The in-plane deformation of WS_2 has led to the increased anisotropy and decreased bandgap.

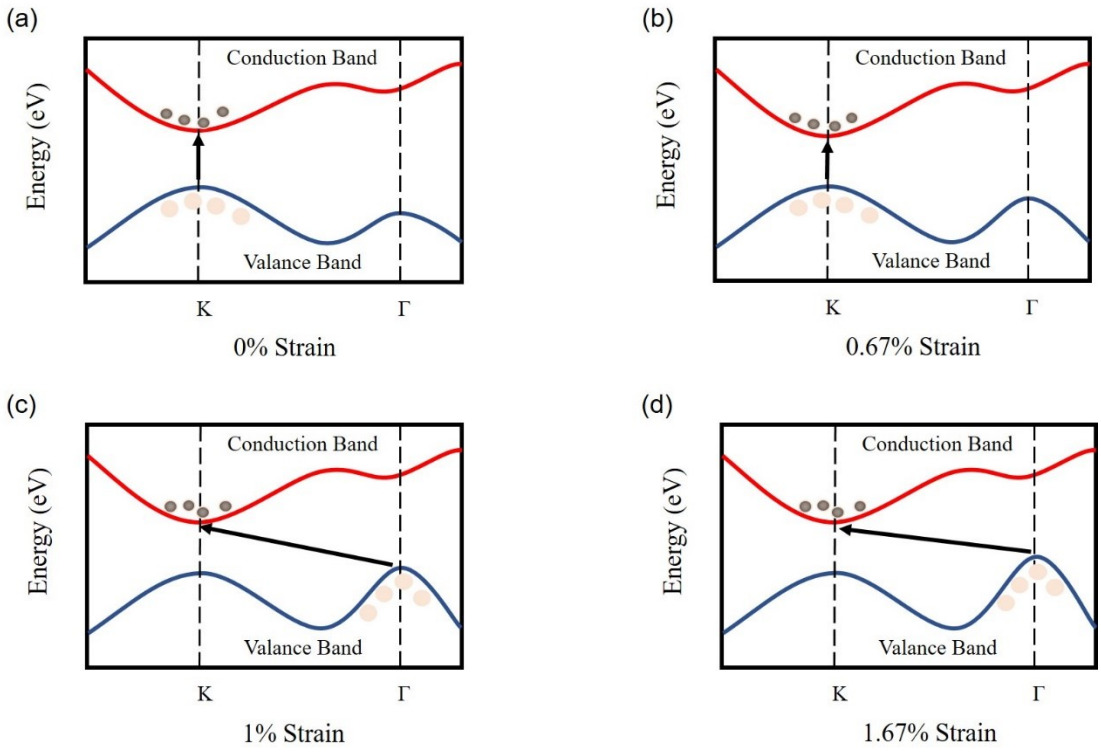

Fig. S7 Evolution of the band structure as the function of the in-plane strain.

In order to understand the changed band structure by in-plane strain clearly, the evolution of the band structure with increased strain is shown in Fig. S7. Without strain, the direct-gap transition is around the K-point of the Brillouin zone, so conduction-band minimum (CBM) and valence-band maximum (VBM) is at the K-point. With the increased strain, the energy of Γ-point in valence band slightly increases. PL spectrum has a redshift due to the reduced bandgap. When the strain is around 1%, with the energy of Γ-point has exceeded the energy of K-point, VBM is moved from K to Γ.[S1] The direct bandgap is transformed to indirect bandgap at this time, which leads to the appearance of I peak. With the strain increases exceeding 1%, the light emission energy from Γ-point of VBM to K-point of CBM is further reduced. Based on previous density functional theory (DFT) calculations, the tungsten d_{z^2} orbitals contribute to conduction and valence band electronic states, causing the direct to indirect band gap transition under the strain.[S2]

The D and I peaks in PL spectra have linear redshift with increased strain, and the redshift rate of D and I are 8.98meV/% and 17.91meV/% strain, respectively. The reason of redshift is that the applied strain increases the bond length of W-S and W-W, so the nuclear potential field experienced by the electrons in the crystal is weaken, which reduces the split effect for energy level. Therefore, bandgap is reduced and orbital hybridization is weakened, which results in a redshift of PL peak.

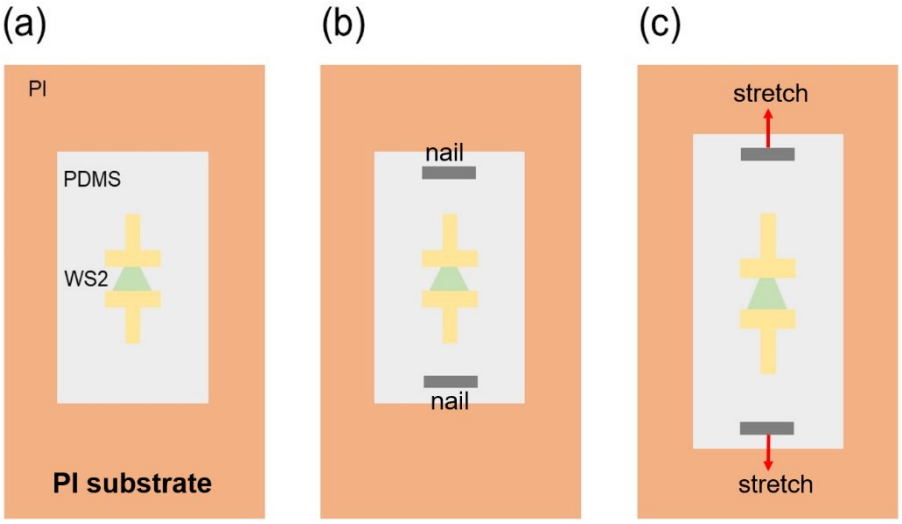

Fig. S8 Schematic diagram of PI substrate with fixed PDMS film for initial state (a, b) and deformed state (c).

To measure the dynamic piezoelectric signal of the deformed monolayer WS_2, we transfer the PDMS film with WS_2 device to the PI substrate as shown in Fig. S8a. The PDMS film is manually stretched and the two sides are fixed on the PI substrate using a nail as shown in Fig. S8b, c. Thus, the in-plane deformation can be fixed by this way. For the measurement of dynamic piezoelectric signal, the PI substrate with fixed PDMS film on top is bended and released periodically.

Table S1 Comparison of piezoelectric current among different 2D materials.

order	materials	current output	References

1	α-In_2Se_3 (2H phase)	47.3 pA (0.76%strain)	Ref. S3
2	Monolayer MoS_2	30 pA (0.64% strain)	Ref. S4
3	Monolayer WSe_2	100 pA (0.39% strain)	Ref. S5
4	Pristine Monolayer WS_2	5 pA (0.25% strain)	This work
5	Monolayer WS_2 with in-plane strain	40 pA (0.25% strain)	This work

Reference

[S1] Wang. Y, Cong. C, Yang. W, Shang. J, Peimyoo. N, Chen. Y, Kang. J, Wang. J, Huang. W and Yu. T, *Nano Res*., 2015, **8 (8)**, 2562-2572.

[S2]R. Chaurasiya, A. Dixit, R. Pandey, *Superlattices and Microstructures* 2018, **122**, 268-279.

[S3]Xue. F, Zhang.J, Hu. W, Hsu, Han. A, Leung. S.-F, Huang. J.-K, Wan. Y, Liu. S, Zhang. J, He. J.-H, Chang. W.-H, Wang. Z. L, Zhang. X and Li. L.-J, *ACS Nano*., 2018, **12**, 4976-4983.

[S4] Wu. W, Wang. L, Li. Y, Zhang. F, Lin. L, Niu. S, Chenet. D, Zhang. X, Hao. Y, Heinz. T. F, Hone. J and Wang. Z. L, *Nature*., 2014, **514 (7523)**, 470.

[S5] Lee. J.-H, Park. J. -Y, Cho. E.-B, Kim.T.-Y, Han. S, Kim. T.-H, Liu. Y, Kim. S, Roh. C.-J, Yoon. H.-J, Ryu. H, Seung. W, Lee. J.-S, Lee. J and Kim. S.-W, *Adv. Mater.*, 2017, 29, 1606667.